Distribution of trace elements between clays and zeolites and aqueous solutions similar to sea water

Article *in* Applied Geochemistry · December 1992

DOI: 10.1016/S0883-2927(09)80076-0

1 author:

Gilles Berger
French National Centre for Scientific Research
152 PUBLICATIONS **6,775** CITATIONS

Chemical Geology, 71 (1988) 297–312
Elsevier Science Publishers B.V., Amsterdam — Printed in The Netherlands

[1]

BEHAVIOR OF Li, Rb AND Cs DURING BASALT GLASS AND OLIVINE DISSOLUTION AND CHLORITE, SMECTITE AND ZEOLITE PRECIPITATION FROM SEAWATER: EXPERIMENTAL INVESTIGATIONS AND MODELIZATION BETWEEN 50° AND 300°C

GILLES BERGER, JACQUES SCHOTT and CHRISTOPHE GUY

Laboratoire de Minéralogie et Cristallographie, Université Paul Sabatier, F-31062 Toulouse Cédex (France)

(Received December 22, 1987; revised and accepted June 22, 1988)

Abstract

Berger, G., Schott, J. and Guy, Chr., 1988. Behavior of Li, Rb and Cs during basalt glass and olivine dissolution and chlorite, smectite and zeolite precipitation from seawater: Experimental investigations and modelization between 50° and 300°C. Chem. Geol., 71: 297–312.

This study investigates experimentally the behavior of Li, Rb and Cs during the hydrothermal alteration of a basalt glass and of forsterite.

The behavior of trace alkalis during the dissolution of a basalt glass and forsterite has been followed between 150° and 300°C: Rb and Cs are preferentially leached from the glass while Li exhibits a stoichiometric release with respect to silica. On the other hand, incongruent loss of Li relative to Si during forsterite dissolution reflects a crystallographic (site energy) control of the release of trace elements from crystalline silicates. The partitioning of Li, Rb and Cs between hydrothermal solutions and chlorites, smectites and zeolites has been experimentally investigated between 50° and 260°C. The alteration phases were synthesized by altering silicate glasses in solutions containing the trace alkalis. The lower the temperature, the higher the exchange capacity of the mineral or the lower the ionic hydration energy, then the more the element is incorporated into the solid phases.

Computer simulations generated with the EQ3/6 software package and our experimental data on distribution coefficients account for the behavior of alkali trace elements during the alteration of basalt glasses by seawater at mid-ocean ridges.

1. Introduction

Knowledge of the distribution of trace elements between hydrothermal solutions and secondary silicate minerals is of primary interest in understanding and modeling the large-scale hydrothermal alteration of the oceanic crust near mid-ocean ridges. Our understanding of the chemistry of reacting hydrothermal systems has been considerably advanced by studies of the present-day mid-ocean ridge hydrothermal systems (e.g., Edmond et al., 1979; Mottl, 1983; Staudigel and Hart, 1983; Michard et al., 1984; Seyfried, 1987). From these and many other studies on hydrothermal ore deposition or geothermal systems, it is clear that trace elements are mobilized because of destruction of their host silicates. Simultane-

0009-2541/88/$03.50

ously, secondary alteration minerals which form, such as chlorites, smectites, zeolites, epidotes, etc., may incorporate some or none of the trace elements just released. Until now, despite much conflicting evidence, studies devoted to modeling hydrothermal alteration have ignored the incorporation in secondary phases of the trace elements released during hydrothermal alteration, largely because of lack of data on the distribution coefficients. It is thus urgent to obtain such quantitative data.

Alkaline elements like Li, Rb and Cs, which are minor constituents of both seawater and rocks and are stable in aqueous solutions (absence of complexation, only one valence state), are good candidates to follow the evolution of hydrothermal systems. Numerous observations of altered oceanic basalts show an important enrichment of secondary phases in Rb and Cs, particularly in the case of low-temperature alteration (Thompson, 1973; Hart et al., 1974; Heinrichs and Thompson, 1976). On the other hand, there have been very few experimental investigations to document this problem. Ellis and Mahon (1964, 1967) have observed during experimental alteration of volcanic rocks at temperatures up to 600°C that the concentration of Rb in solution is controlled by the precipitation of secondary phases, while Li and Cs largely accumulate in solution. Seyfried et al. (1984) have investigated experimentally Li and B behavior during alteration of basalt glass and diabase by seawater at 150° and 375°C. They brought to light the role of temperature on Li behavior: it is leached from the solid at 375°C, but is incorporated in secondary phases at 150°C. These experiments have shown interesting trends; however, they neither distinguish the pure dissolution stage from the precipitation of secondary phases, nor do they permit quantification of the distribution of trace alkalis.

The elemental processes which control the hydrothermal dissolution of glasses have been recently characterized by Berger et al. (1987) in a study limited to the behavior of major elements and Li. Data on the partition of alk between silicates and hydrothermal soluti are available only for micas and feldspars [cite and orthoclase (Lagache, 1968, 19 nepheline and albite (Roux, 1971); sanid muscovite and phlogopite (Volfinger, 1 1974, 1976); alkali feldspars (Lagache and batier, 1973; micas and feldspars (Volfinger Robert, 1980)].

In the present study we have investigated perimentally the behavior of Li, Rb and Cs ing the hydrothermal alteration of a basalt g and of forsterite. In dissolution experim carried out between 150° and 300°C we determined the distribution coefficients o kalis between hydrothermal solutions and cate phases representative of sea- alteration from 50° to 260°C. Finally, the sured distribution coefficients have been with the EQ3/6 computer software packa simulate the behavior of alkali elements du the alteration of a basalt glass by seawate

2. Methods

Experiments have been conducted in orc characterize the behavior of alkalis durin hydrothermal dissolution of a basalt glas riched in Li, Rb and Cs and of a forsterit riched in Li. Run times were less than a c order to avoid the precipitation of seco phases.

The distribution coefficients of Li, Rb a have been measured between hydrotherm lutions and the silicate phases (chlorites, tites, zeolites) which precipitate durin experimental alteration of synthetic si glasses by seawater-type solutions. The positions of both the reacting solution glasses have been chosen in order to allo precipitation of selected solid phases. The alkalis were initially contained only i aqueous solution.

2.1. Starting materials

2.1.1. Dissolution experiments

Silicate glasses were prepared by mixing known amounts of reagent grade basic oxides, and aluminosilicates in the case of Rb and Cs. The powdered mixtures were melted at 1500°C in Pt crucibles, cooled and cast into slabs. The slabs were allowed to react with a 10^{-4} *M* HCl solution.

A fine-grained crystalline Li-Sc-forsterite was synthesized at 1550°C by reaction of a mixture of reagent grade SiO_2, MgO, Sc_2O_3 and Li_2O in a Pt crucible. The electrical charge deficit resulting from the Li–Mg substitution was balanced by an equivalent Sc–Mg substitution [the solid-solution series $(Li,Sc)SiO_4$–Mg_2SiO_4 has been studied by Ito (1977)]. The crystallinity and the chemical homogeneity of the synthesized forsterite were observed by X-ray diffraction (XRD) and electron microprobe analysis. The synthetic crystals were 3–10 μm in size (specific area was found to be 8000 $cm^2\ g^{-1}$) and they were used without preliminary treatment. The runs were conducted in synthetic seawater from which Mg^{2+} and SO_4^{2-} were removed in order to follow the release of Mg in solution and to avoid precipitation of sulfates (this solution can be viewed as a highly reacted hydrothermal fluid).

2.1.2. Partitioning experiments

Silicate glasses were prepared as described above (but without trace alkalis) and ground with an agate mortar and pestle. The 135–360-μm fraction was separated by dry sieving. In order to remove ultrafine particles produced by grinding, the grains were treated with an ultrasonic cleaner in distilled water (Branson® Sonifer B-*30*).

The compositions of both solutions and glasses have been chosen in order to allow the precipitation of one of the following silicates:

Smectites. The glass had a basaltic composition and the starting solution composition was close to that of seawater. The solution was prepared according to Kester et al. (1967) for the 50–100°C runs; for the 150–260°C runs, pH and Mg^{2+}, Ca^{2+} and SO_4^{2-} concentrations were lowered in order to avoid precipitation of anhydrite and magnesium oxysulfate during heating [this was done in the light of Bischoff and Seyfried's study (1978)];

Chlorites. For the 150–260°C runs, the starting materials were the same as above; for the 50–100°C runs, the glass was an Al_2O_3–MgO-rich/SiO_2-poor glass and the starting solution was distilled water;

Zeolites. The starting materials were a sodic silicate glass and a 0.428 *M* NaCl solution. The initial pH was raised to 10 by addition of NaOH.

The chemical compositions of the starting materials are reported in Table I.

2.2. Experimental procedure

The dissolution experiments were carried out in a hydrothermal apparatus as described in Berger (1987), at 200° and 300°C for the basalt glass, and at 150°, 200° and 260°C for forsterite. It consists of a Pt reactor inserted into a steel Prolabo® pressure vessel, heated by an electric furnace and agitated by rocking the entire assemblage. The initial surface area/solution volume ratios were $1.5 \cdot 10^{-2}$ and $6 \cdot 10^{-4}$ cm^{-1} for the basalt glass at 200° and 300°C, respectively, and 5 cm^{-1} in the case of forsterite. For each experiment, three aliquots of the solution were taken during the run, filtered through a 0.2-μm Millipore® filter and then analyzed for both major and trace elements. Dissolved SiO_2 and Al were analyzed spectrophotometrically as silicomolybdate and by the Catechol method described in Dourgan (1974), respectively. Fe, Li, Rb and Cs were analyzed by flame spectrophotometry (Perkin-Elmer® *5000* spectrophotometer); Mg and Ca were determined by ion chromatography (Dionex® *2000*i ion chromatograph). The pH of the re-

TABLE I

Chemical composition of the starting materials

(a) Solids (wt.%)

Run/T (°C)	SiO_2	Al_2O_3	FeO	MgO	CaO	Na_2O	K_2O	B_2O_3	Li_2O	Rb_2O	Cs_2O	Sc_2O_3
Mg-smectite/50-260	48.4	14.6	11.2	6.9	11.1	2.7	0.1	5.0	–	–	–	–
Ni-chlorite/150-260	48.4	14.6	11.2	6.9	11.3	2.7	0.1	5.0	–	–	–	–
Mg-chlorite/50-100	30.0	16.3	–	33.7	–	–	–	20	–	–	–	–
Na-zeolite/150-260	60.4	21.1	–	–	3.8	9.5	–	5.0	–	–	–	–
Na-zeolite/50-100	38.2	19.3	–	–	–	36.2	–	10	–	–	–	–
Glass dissolution	45.5	13.9	9.7	4.5	8.9	2.8	–	–	3.68	2.56	2.41	–
Forsterite dissolution	44.6	–	–	54.2	–	–	–	–	0.35	–	–	1.58

(b) Solutions (10^{-3} m)*

Run/T (°C)	Cl^-	HCO_3^-	Na^+	Mg^{2+}	Ca^{2+}	SO_4^{2-}	K^+	pH
Mg-smectite/150-260	545	2.33	468	49	1.35	16	9.9	4
Mg-smectite/50-100	545	2.33	468	53.3	10.1	28	9.9	7.8
Ni-chlorite/150-260	545	2.33	468	49	1.35	16	9.9	4
Mg-chlorite/50-100				distilled water				
Na-zeolite/50-260	428	–	428	–	–	–	–	10
Glass dissolution	0.1	–	–	–	–	–	–	4
Forsterite dissolution	522	2.38	465	–	25	–	9.9	4

*Trace alkali concentrations are reported in Table III.

acting solution was measured at 25°C immediately after sampling. A fourth sample was taken at the end of the experiments after quenching the solution to check that no silicate phases precipitated during cooling. Results were corrected for increases in solid/solution ratio (up to 20%), due to the removal of solution samples for analyses, by calculating the mass of dissolved species prior to each sampling and normalizing to the initial volume.

For the synthesis of each type of secondary silicate phase, several sets of experiments were performed under vapor pressure at 50°, 75°, 100°, 150° and 260°C, and during various times ranging from 4 days (at 260°C) to 3 months (at 50°C). The initial solution/glass mass ratios were 50 at 150° and 260°C, and between 2 and 10 at lower temperatures. These water/glass ratios were chosen in order to keep the concentration of trace elements in solution roughly constant during the experiments. At 50° and 75°C the runs were conducted in tight, closed polypropylene bottles, whereas at 100°C they were carried out in Teflon® reactors. The bottles and reactors were placed in an oven at constant temperature. At 150° and 260°C the distribution experiments with smectites and zeolites were conducted in the Pt reactor. For the chlorite runs at 150° and 260°C the glass alteration was carried out in a nickel-plated autoclave because preliminary runs showed that Ni promoted chlorite formation at the expense of smectite.

For each type of secondary silicate and each chosen reaction temperature we carried out several runs with various amounts of trace alkalis in the starting solution. At the end of each run the concentrations of trace alkalis in solution were measured in order to check if they have remained constant.

2.3. Solid analysis

After each partitioning run, in order to recover the secondary silicates, the altered glass grains were suspended in distilled water and treated with a high-energy ultrasonic cleaner. The glass grains were separated by decantation. The secondary phases were recovered by filtration of the solution, rinsed with distilled water, dried at 40°C and identified by XRD. Then, after a triacid attack (HF, HNO_3, $HClO_4$), the recovered secondary silicates were analyzed by flame spectrometry for Li, Rb, Cs, Na, K, Ca, Mg, Fe and Al. Because of the use of hydrofluoric acid, SiO_2 content could not be determined. The small amount of secondary phases produced during the runs (20–50 mg) did not allow total chemical analysis using more specific methods such as microprobe or X-fluorescence.

2.4. Computer programs

In order to model the behavior of trace alkalis during basalt hydrothermal alteration, basalt–seawater interactions have been simulated at 50° and 260°C using the EQ3/6 computer code developed by Wolery (1979, 1983). EQ3 computes the equilibrium distribution of species in the aqueous solution, generates concentrations and activities of ions and complexes, and calculates the index of saturation of mineral phases with respect to the solution. EQ6 calculates chemical equilibria and mass transfer in aqueous solution–mineral systems utilizing a step-wise procedure involving titration of increments of solid phases into the solution. Product phases may remain in the equilibrium system ("closed-system" model) or may be removed as formed ("open-system" model). The calculations presented here are for a "closed system". The thermodynamic data of the minerals, aqueous species and water are provided by the SUPCRIT program developed by Helgeson et al. (1978, 1981). Relative reaction rates of the reacting minerals are specified in the calculations described above by evaluating, at each step of reaction progress, an appropriate statement of the dissolution equation using specified values of the rate constants.

3. Results

3.1. Dissolution

The basalt glass dissolutions lead to the formation of an iridescent and fragile altered skin. Its thickness reaches 50 μm at 300°C. No crystallized phase has been identified within this skin by XRD or scanning electron microscopy. Its chemical composition has been determined by microprobe analysis on polished sections of the altered slabs and is reported in Fig. 1. In the light of our previous study on the processes controlling the hydrothermal dissolution of basalt glasses (Berger et al., 1987) and of the el-

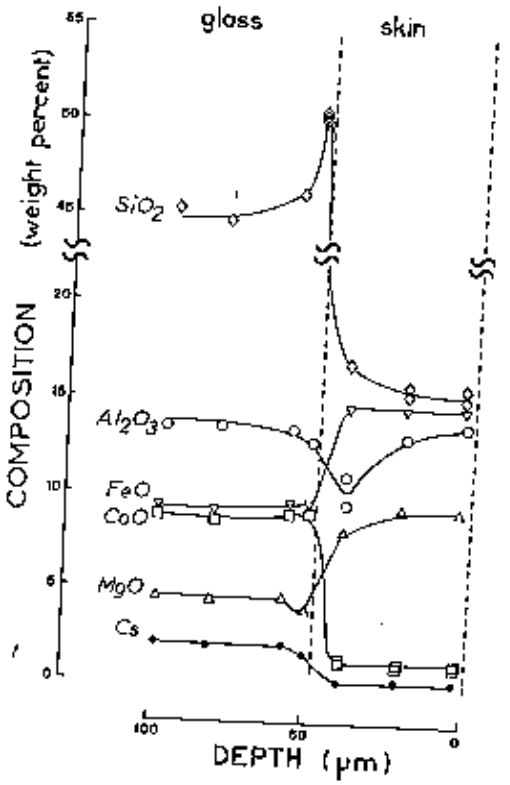

Fig. 1. Microprobe analyses of slabs of glass reacted at 300°C.

TABLE II

Kinetics of glass dissolution at 200° and 300°C

Temperature (°C)	Time (hr.)	SiO_2	Li	Rb	Cs	Mg	Ca	pH
		(10^{-7} mol cm^{-2})						
200	3	105	37.7	3.8	2.9	25	27	3.5
	10	337	114	12.5	7.8	40	52	3.7
	21	399	227	21.8	13.3	30	95	4.1
300	0.5	459	118	26.2	14.7	65	–	3.6
	2	764	236	52.5	22.9	147	246	3.8
	3.5	983	331	62.3	37.7	65	311	3.7

emental microprobe profiles at the glass–skin boundary (increase of Si, decrease of Al, Cs and Mg), this skin appears to be a residual hydrated silicate gel which results from the non-stoichiometric dissolution of the glass. The chemical analyses of the solutions (Table II) reflect the formation of the residual gel (non-linear release of Si, initial increase and decrease of Mg in solution, etc.). The behavior of alkalis during the first stage of dissolution at 300°C is presented in Fig. 2a and compared to a stoichiometric release with respect to silica. Rb and Cs present a preferential release (in agreement with the Cs microprofile in the glass near the glass–skin boundary) while the release of Li appears to be stoichiometric with respect to silica. At 200°C the non-stoichiometric releases of Rb and Cs ar less marked.

The dissolution of forsterite, as that of basalt glass, is characterized by a strong preferential release in solution of cations with respect to silica. As an example, our experimental results at 260°C are reported in Fig. 2b. It is interesting to note that Li exhibits a marked incongruency with respect to silica, in contrast to its behavior during glass dissolution. Note also that Li release is stoichiometric with respect to Mg. This cation behavior is not due to the precipitation of secondary silicates: we checked with the EQ3 program that no secondary silicate precipitated during the runs. From chemical analysis of the solution it can be deduced that the thickness of

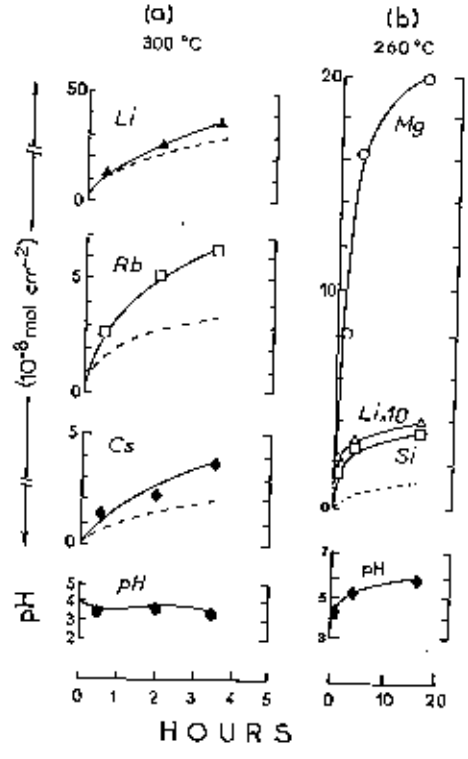

Fig. 2. a. Release of alkalis to solution during glass dissolution at 300°C, compared to stoichiometric release with respect to silica (*dashed lines*).
b. Rate of dissolution of the Li-forsterite at 260°C, compared with stoichiometric release of Li with respect to Si (*dashed line*).

the Li–Mg-leached layer reaches 300 Å after only 16 hr. of dissolution at 260°C.

3.2. *Partitioning*

The zeolite runs led to the precipitation of analcime at 260°C, analcime with small amounts of Na-phillipsite (A.S.T.M. ref. *12-195*) at 150°C, and of a Na-chabasite–analcime–Na-phillipsite mixture at 100°, 75° and 50°C. The chlorite runs led to the formation of a Ni-rich chlorite (17% Ni on the average) at

260° and 150°C, and of poorly crystallized clinochlore at 100°, 75° and 50°C. The smectite runs led to the formation of well-crystallized saponite at 260°C, and of poorly crystallized saponite at 150°C. No diffraction patterns were detected for the phases formed at 100°, 75° and 50°C.

The chemical compositions of these secondary silicates for both major elements and trace alkalis are given in Table III together with the concentrations of trace alkalis in the reacting solutions. During synthesis of smectites and chlorites, the small amount of altered phases which formed did not modify the initial alkali concentration of the solutions. But in a few zeolite runs the solutions lost up to 60% of their initial alkali content. For these runs we took the final solution concentrations into account, assuming that the whole alteration phase was in equilibrium with the final solution.

For each temperature and each type of solid phase, when the concentration in the solid of a given alkali is plotted vs. the concentration in solution, the representative points fall on a straight line which passes through the origin. This correlation reflects equilibrium between the solution and the secondary phases, and indicates that the alkali distribution obeys the Berthelot–Nernst law. As an illustration, Fig. 3 gives the partitioning of Cs between solution and zeolites. For each silicate phase, the distribution coefficient D has been defined as the ppm concentration of the trace in the solid over that in the solution. The experimental results are reported in Table IV. Note that the distribution coefficients in this way defined are not truly thermodynamic and may take into account several elementary processes (adsorption on the surface, exchange with the compensating cations, substitution within the lattice, etc.) which we did not try to separate; we considered that the global values for D are more representative of the natural processes that we investigated. Moreover, these distribution coefficients should be viewed as more representative of a mineralogical structure than of a single mineral.

4. Discussion

4.1. Behavior of alkalis during basalt glass and forsterite dissolution

In a previous study on the alteration of a basalt glass by seawater (Berger et al., 1987) we have shown that dissolution is controlled by diffusion of dissolved species through an altered layer. Selective removal of cations (Na, Ca, Mg, Fe), except Li, leads to the formation of a thick, porous protonated surface enriched in SiO_2. The same mechanisms control the dissolution experiments reported in this study. We found again a stoichiometric release of Li with respect to silica. This affinity of Li for the glass network has been already pointed out by Garofalini and Levine (1985) which evidenced by molecular dynamics considerations that localized surface re-arrangements occur after formation of free surfaces, favoring the release of Na and K but not that of Li.

By contrast, the dissolution experiments of forsterite illustrate the structural control of crystalline silicates on the release of trace elements. During forsterite dissolution, Li and Mg, which occupy the same structural site, undergo the same preferential release. Such crystallographic control of cation release during silicate mineral dissolution has been already demonstrated by Schott et al. (1981) and Schott and Berner (1983) for pyroxenes and amphiboles. They explained the incongruent losses of Ca in diopside and tremolite, Mg in enstatite and Fe in bronzite, in terms of the lower Madelung energies of M_2 sites (and M_4 sites in tremolite) relative to M_1 sites.

Preferential leaching of alkalis from olivines, pyroxenes and feldspars due to lattice-structural control may strongly affect the chemical composition of hydrothermal solutions in the case of high water/rock ratios. However, in the case of low water/rock ratios, this process is likely to have little effect because the excess of alkalis lost by minerals will be negligible with regard to the amount congruently released.

TABLE III

Chemical composition of the secondary phases and alkali concentrations of the reacting solutions

Temperature, T (°C)	Smectites							Solution		
	Al_2O_3 (wt.%)	FeO	MgO	CaO	Li (ppm)	Rb	Cs	Li (ppm)	Rb	Cs
50	10.9	10.1	6.1	5.0	24	380	692	10	50	50
	10.2	11.3	6.2	4.4	10	475	729	5	75	75
	11.1	11.9	5.5	4.6	8	881	1,326	1	100	100
75	11.5	13.0	5.2	4.5		407	590		50	50
	11.1	13.5	6.0	4.7		619	806		75	75
	11.0	12.2	6.3	5.2		850	1,330		100	100
100	13.2	15.4	5.7	4.8		170	300		25	25
	12.7	14.3	5.9	5.0		440	649		50	50
	13.0	14.7	5.9	4.2		798	–		100	75
150	13.2	12.0	26.9	3.1	3	–	–	0.2	–	–
	12.2	13.4	16.9	2.7	52	<10	<10	10	1	1
	15.6	12.8	15.6	2.8	82	430	520	50	50	50
	9.71	13.9	16.8	3.6	276	230	1,551	100	30	100
260	16.2	10.4	24.2	3.0	3	–	–	0.2	–	–
	12.0	10.1	19.8	1.8	3	–	–	0.5	–	–
	13.3	8.96	20.1	3.5	27	–	–	10	–	–
	11.5	10.0	19.5	2.4	24	<10	–	10	1	–
	12.2	9.03	17.9	0.9	70	300	<10	40	50	1
	14.6	10.5	14.3	1.4	89	80	410	50	10	50
	12.3	9.92	13.8	1.8	195	610	760	100	100	100

Temperature, T (°C)	Chlorites							Solution		
	Al_2O_3 (wt.%)	FeO	MgO	NiO	Li (ppm)	Rb	Cs	Li (ppm)	Rb	Cs
50	15.6		27.1		15	210	300	10	100	100
					11	160	210	5	75	75
					<2	90	170	1	50	50
					–	30	50	–	10	10
75	13.9		28.4			180	210		100	100
						150	180		75	75
						70	70		50	50
100	15.4		27.9			<10	<10		10	10
						130	180		100	100
						90	140		75	75
						80	80		50	50
150	9.2	11.3	8.7	29.0		<10	<10		10	10
	8.3	7.8	20.4	18.5	2	–	–	0.2	–	–
	10.6	8.7	6.72	29.1	16	12	<10	10	10	1
260	11.8	10.2	6.92	19.2	67	108	45	100	100	50
	14.8	13.4	19.1	11.1	63	206	120	70	200	100
	7.11	11.6	13.9	18.3	3	–	–	0.2	–	–
	10.1	10.2	6.64	26.2	4	14	–	10	10	–
	6.8	14.3	18.2	14.6	30	105	<10	50	200	1
	10.1	8.53	11.0	21.0	20	43	37	100	100	100
					43	62	149	200	200	200

TABLE III (*continued*)

Temperature, T (°C)	Zeolites						Solution		
	Al_2O_3 (wt.%)	Na_2O	CaO	Li (ppm)	Rb	Cs	Li (ppm)	Rb	Cs
50	17.2	18.2		240	1,304	6,366	8	4.3	2.6
	16.4	21.3		176	554		4.5	1.8	
	17.8	20.5		22	296	1,021	0.8	0.7	0.5
76	17.2	20.9			1,835	7,914		6.3	4.9
	17.6	21.4			985	4,623		3.6	2.6
	17.8	20.4			516	2,062		2.0	1.2
100	17.8	20.9			1,643	6,061		5.8	6.8
	20.2	21.9			1,009	2,738		4.2	2.8
	18.9	22.1			529	1,629		2.0	1.5
150	30.53	33.16	0.08	9	183	1,458	1	1	0.9
	26.8	43.25	0.19	4	88	344	0.5	0.5	0.5
260	19.81	21.9	3.44	48	954	1,912	10	8	5
	21.86	27.13	1.3	10	352	1,660	5	4	3
	21.68	21.18	0.26	2	101	422	1	1	0.5

4.2. Distribution coefficients

Because alkali elements are hydrated in solution, the energy associated with the exchange reaction is the difference between the site energy of the alkali in the solid phase and its hydration energy in solution. Hydration energies of alkalis are well known: according to Latimer et al. (1939), the free energies of hydration at 25°C of Li^+, Rb^+ and Cs^+ are -479.5, -282.5 and -254 kJ mol^{-1}, respectively. As expected, our data show that the smaller the absolute value of the free energy of hydration, the more easily the cation is incorporated into the solid phase (in other words, the higher the distribution coefficient). This increasing incorporation of alkalis from Cs to Li into clay structure is in agreement with trace-element analyses in fresh and altered sea-floor basalts (Tlig, 1982; Staudigel and Hart, 1983).

The various site energies in clay minerals are poorly known, but as inferred by Goldschmidt's rules and Volfinger and Robert (1980) they are roughly proportional to the difference Δ between the radius of the cavity effectively occupied in the mineral structure and the radius of the trace cation. In other words, the smaller Δ, the greater the tendency for the cation to enter the structure. This hypothesis, which supposes true substitution in the lattice, cannot be applied to most of our experiments because Rb and Cs are too large to be substituted for Mg in the octahedral sites of chlorites and smectites ($r_{Cs}=1.82$ Å, $r_{Rb}=1.68$ Å and $r_{oct.site}=0.97$ Å) or for Na in the zeolites ($r_{zeol.site}=1.10$ Å). Obviously, in chlorites and smectites Rb and Cs are located in interlayer positions whereas in zeolites they occupy vacancies of the lattice (see Passaglia, 1978). In support of this hypothesis it should be emphasized that for a given cation, the distribution coefficients for the different clay structures rank in the same order as the exchange capacities (Table V). By contrast, Li which has a smaller ionic radius ($r_{Li}=1.00$ Å) can be located either in interlayers or substituted for Na in zeolites or for Mg and Fe in the octahedral sites of chlorites and smectites.

A plot of the logarithm of the measured dis-

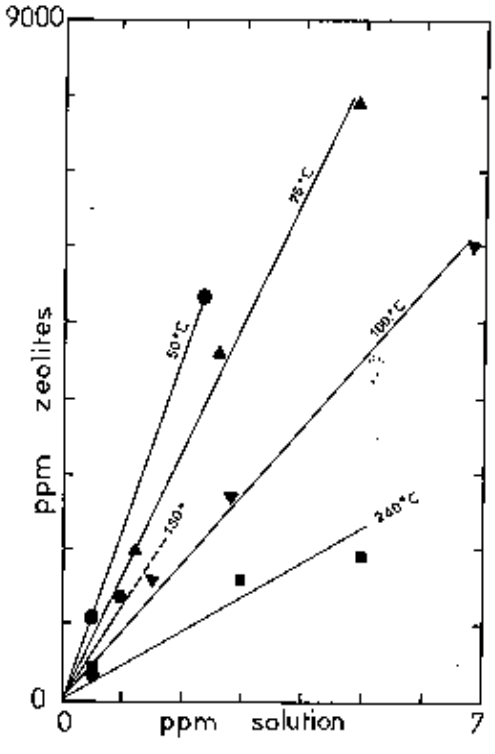

Fig. 3. Plot of Cs concentration in zeolites vs. concentration in solution.

TABLE IV

Distribution coefficients of Li, Rb and Cs between solutions and alteration phases

Mineral	Temperature, T (°C)	$D_{mineral/solution}$ (ppm ppm^{-1}) Li	Rb	Cs
Chlorites	50	1.7 ±0.2	2.0±0.1	3.0±0.5
	75		1.7±0.2	2.0±0.4
	100		1.4±0.2	1.75±0.15
	150	0.8 ±0.1	1.0±0.1	1.05±0.15
	260	0.35±0.10	0.4±0.1	0.55±0.2
Smectites	50	2.4 ±0.1	7.5±1	12±2
	75		8.3±0.2	12±1.3
	100		8.0±1	12.5±0.5
	150	2.3 ±0.3	8.1±0.5	13.5±2.5
	260	1.9 ±0.3	5.6±0.5	8.0±0.5
Zeolites	50	33 ±5	315±15	2,084±50
	75		274±15	1,700±200
	100		255±10	985±100
	150	8.5±0.5	180±4	1,000±300
	260	3.5±1.5	110±10	440±100

TABLE V

Order of magnitude of the exchange capacity of synthesized minerals

	EC (meq/100 g)	Reference
Chlorites	10–15	[1]
Saponite	50–60	[1]
Analcime	450	[2]

References: [1] = Caillère et al. (1982); [2] = Barrer (1978).

tribution coefficient against the reciprocal of temperature (Arrhenius diagram) is shown in Fig. 4. Except for smectites at low temperatures, the distribution coefficients of the three

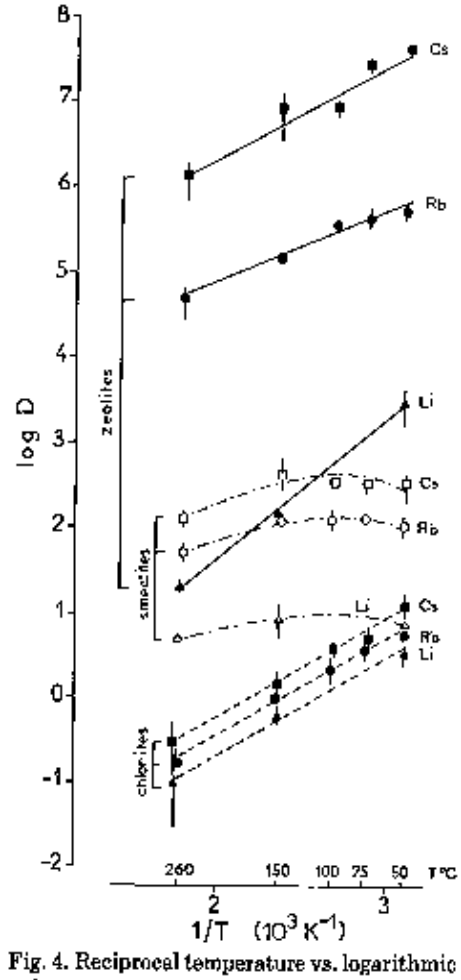

Fig. 4. Reciprocal temperature vs. logarithmic value of distribution coefficient of alkalis (Arrhenius plot) between solution and secondary phases.

alkalis decrease with increasing temperature. For chlorites and zeolites, the linear relationships between log D and $1/T$ indicate that the enthalpies of reactions are constant between 50° and 260°C. In the case of smectites, the distribution coefficients increase from 260° to 150°C, but remain constant at lower temperature. These latter data may reflect either the poor crystallinity of these products or an evolution of the clays towards an interstratified chlorite-smectite structure.

The effect of temperature on the distribution coefficients is the opposite of that generally observed when true substitution occurs within the solid lattice. For example, in the temperature range 400–800°C, Volfinger (1976) has shown that the affinity of Na, Rb and Cs for sanidine, muscovite and phlogopite increases with increasing temperatures. The temperature control of alkali distribution as evidenced in our experiments confirms that our data reflect, rather than a true substitution, an exchange reaction with the compensating cations of the minerals. Moreover, one understands that the exchange capacity of the solids increases with decreasing temperature because the poorly crystallized solid phases synthesized to low temperatures offer more crystallochemical defects and vacancies, and because adsorption of cations is facilitated by a decrease of thermal agitation. It is likely that the distribution of trace alkalis during the alteration of basalt glass by seawater at mid-ocean ridges is controlled by the same mechanisms. Indeed, recent observations show that the alteration of the oceanic crust at high temperature (350°C) released alkalis in solution, whereas at lower temperature these elements are incorporated in altered phases (Edmond et al., 1979; Saunders et al., 1979; Seyfried et al., 1984; Stoffyn-Egly and MacKenzie, 1984).

5. Simulation of the behavior of Li, Rb and Cs during the alteration of a basalt glass by seawater

These simulations have been generated at 50° and 260°C using our experimental data and the EQ*3/6* computer software package.

The basalt glass has a tholeiitic composition and its alkali content is 7 ppm for Li, 3 ppm for Rb and 0.05 ppm for Cs. The starting solution is standard seawater which contained 0.18 ppm of Li, 0.12 ppm of Rb and 0.0004 ppm of Cs (from Martin and Whitfield, 1983). We did not take into account the preferential release of Rb and Cs from the glass because these simulations deal with low water/rock ratios.

The procedure of our simulations was as follows:

In a first stage, the secondary mineral assemblage has been determined using the EQ*3/6* programs. Among the secondary phases obtained in a preliminary run, numerous phases like garnets, epidotes, feldspars, pyroxenes, amphiboles, wollastonite, lawsonite, prehnite and micas (muscovite, phlogopite, paragonite) do not normally form in this range of temperature and pressure. Accordingly, these phases have been prevented from forming in the simulations presented here. The nature and the mass of the secondary phases which precipitated in our simulations are reported in Fig. 5 as a function of the mass of dissolved glass per kg of solution (or solution/rock ratio). In the case of chlorites, smectites and zeolites the solid phases are regrouped according to their mineralogical structure. The phases which precipitated in small amounts are named "minor phases".

In a second stage, the amount of alkalis available in the system (mass initially present in solution plus that released by glass dissolution) was distributed between the solution and chlorites, smectites and zeolites using our measured distribution coefficients (Table VI). The "minor phases" (mainly carbonates, sulfates and oxides) do not represent efficient traps for Li, Rb and Cs, and were ignored in these calculations. The distribution of trace elements was carried out assuming chemical equilibrium between the reacting solution and the considered solid phases. At each step of the reaction progress (increment of basalt glass added sto-

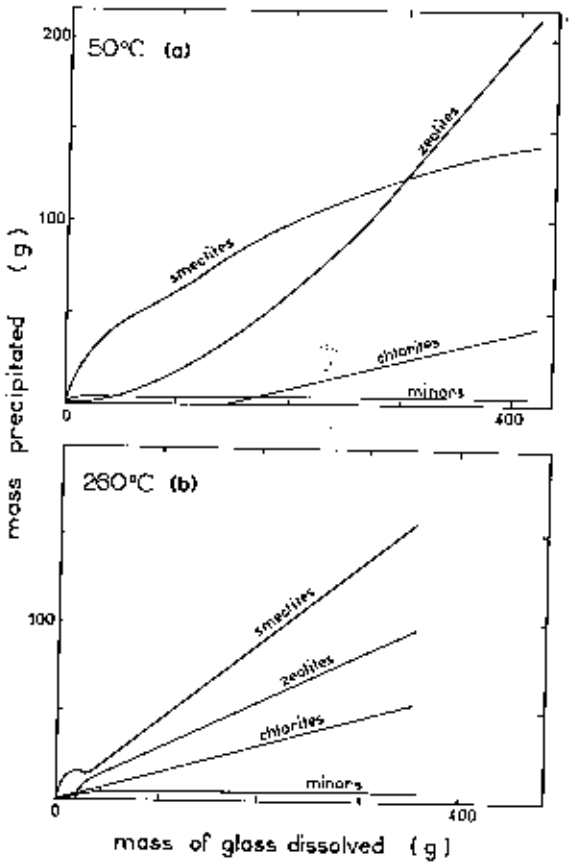

Fig. 5. Identity and amount of minerals calculated to precipitate at 50° (a) and 260°C (b) from 1 kg of solution, as a function of the mass of glass dissolved.
a. *Minors* = gypsum, calcite, pyrite, dolomite, gibbsite, kaolinite, hematite; *zeolites* = analcime, laumontite; *smectites* = saponite, nontronite; *chlorites* = daphnite.
b. *Minors* = anhydrite, calcite, pyrite, margarite, hematite, magnesite, crysotile; *chlorites* = clinochlore, daphnite, amesite; *smectites* = saponite, beidellite, nontronite; *zeolites* = laumontite, analcime.

ichiometrically to the solution), mathematical expressions describing mass action, mass balance, charge balance and non-ideality were solved by EQ3/6 for major elements while mass conservation and distribution of trace elements was solved, using a second computer program, from the mass conservation expression:

$$C_i^0 m_s + X_i^0 m_v = C_i m_s + \sum m_\phi D_i^\phi C_i$$

TABLE VI

Distribution coefficients used in the simulations

Mineral	Temperature, T (°C)	$D^{\text{solid/solution}}$ (ppm ppm^{-1})		
		Li	Rb	Cs
Chlorites	50	1.7	2.1	3
	260	0.35	0.4	0.55
Smectites	50	2.3	7.5	13
	260	1.9	5.5	8
Zeolites	50	33	315	2,064
	260	3.5	110	440

where m_s, m_v and m_ϕ = mass of the solution, of dissolved glass and of phase ϕ precipitated, respectively; X_i^0 = concentration of trace element i in the glass; C_i^0 and C_i = concentration of i in the solution before and after distribution, respectively; and D_i^ϕ = distribution coefficient of i for the phase ϕ. As D_i^ϕ is not truly thermodynamic, this procedure implies that the chemical composition of seawater is quite invariant, which is effectively the case.

Two scenarios were considered. In the first one, at each step of the reaction progress, dissolved trace elements equilibrate with the bulk solid phase which has already precipitated (solid diffusion is allowed), while in the second scenario, trace elements equilibrate only with the solid which has precipitated during the increment of reaction progress considered (solid diffusion is not allowed). It is likely that distribution of alkali occurs within these two ways of limiting behavior.

Calculated trace alkali concentrations in solution are reported in Fig. 6 against the mass of dissolved glass. The two scenarios (solid lines and dashed lines) gave qualitatively the same results; quantitative differences concern mainly the low water/rock ratio but do not exceed 35%.

Rb and Cs present very similar behavior: after a marked transient maximum their concentration in solution tends to reach a steady state.

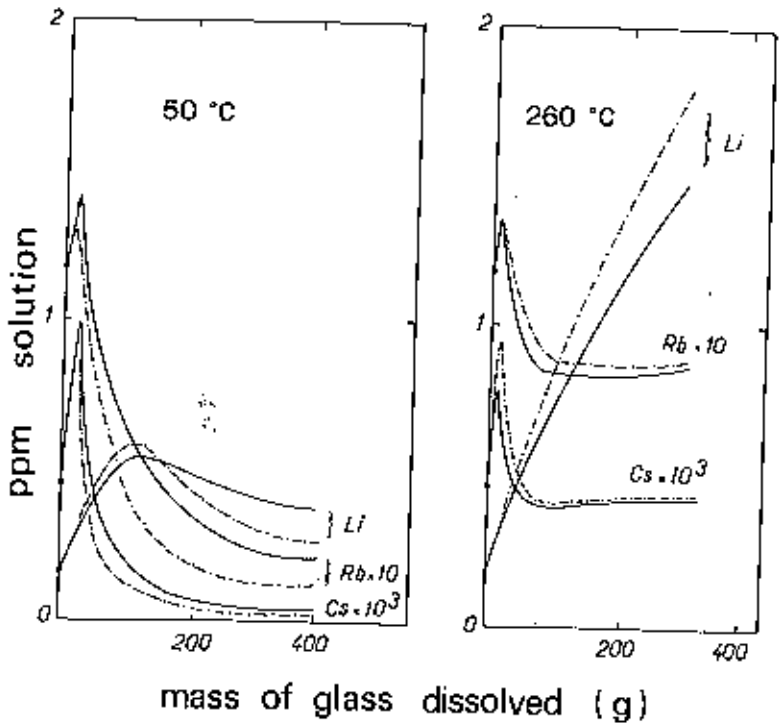

Fig. 6. Calculated concentration of trace alkalis in reacting seawater vs. the mass of glass dissolved per kg of solution (*solid lines*=equilibrium is assumed between solution and the bulk solid phases; *dashed lines*=trace alkalis are not allowed to react with the phases which have already precipitated).

For low water/rock ratios the concentrations at steady state depend only on temperature. At 50°C the solution is impoverished in Rb and Cs (the final concentrations represent 8–20% of the initial values) whereas at 260°C, Rb and Cs concentrations stay roughly constant.

At 50°C Li exhibits the same behavior as Rb and Cs: after an initial increase, Li concentration in solution reaches a steady state for which the amount of Li released by the glass is balanced by the amount incorporated in the secondary phases. By contrast, at 260°C Li concentration regularly increases with the mass of glass dissolved (or the water/rock ratio), reflecting a strong leaching of this element during the glass weathering. These results are in good agreement with the experimental observations of Seyfried et al. (1984). These authors have measured the amount of Li and B release in solution during basalt and diabase–seawater interaction at 150° and 350°C and for several water/rock ratios. They found, at 150°C, a decrease of Li concentration in solution after an initial increase, and a "soluble" behavior at 350°C. In the light of our simulations, the "turnaround" observed by Seyfried et al. at 150°C may be explained by successive precipitations of different silicate phases.

Several authors (Edmond et al., 1979; Michard et al., 1984; Von Damm et al., 1985) reported the chemistry of fluids from submarine hot springs along the Atlantic and Pacific ridges. At 350°C, the alkali contents of fluids range from 4 to 8 ppm for Li, 0.5 to 2 ppm for Rb and are <5 ppb for Cs (Cs concentration is under the detection limit). The Li, Rb and Cs concentrations from our simulations rank in the same order, but are slightly lower than those reported above for Li and Rb. This is probably due to the lower temperature of our simulations, but it may also reflect in these hot springs the existence of water/rock ratios lower than unity, or a basal-

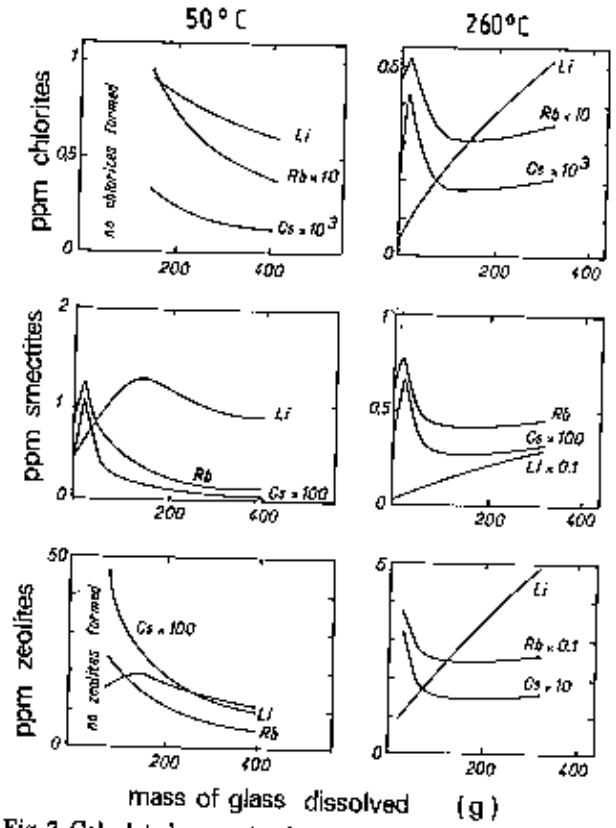

Fig. 7. Calculated concentration of trace alkalis in the secondary phases against the mass of glass dissolved per kg of solution.

tic substrate characterized by Li and Rb concentrations greater than those chosen in our experiments.

In Fig. 7 trace alkali concentrations of chlorites, smectites and zeolites are reported, assuming that at each step of the reaction progress trace elements equilibrate with the bulk solid phase. Except for Li at 260°C, the incorporation of alkalis in the solid increases with the water/rock ratio. The same picture, with small differences, is observed when trace elements equilibrate only with the phases which have precipitated during the increment of the reaction progress considered. In all cases, chlorites and smectites exhibit alkali concentrations lower than that of the starting basalt glass, while zeolites are significantly enriched in Rb and Cs. At 50°C, the maximum concentrations of Rb and Cs (24 ppm Rb and 0.47 ppm Cs) are closed to that reported by Tlig (1982) in analcime formed during the low-temperature alteration of pillow-lava (26 ppm Rb and 0.82 ppm Cs). In this way, the numerous observations of altered basalts which show an enrichment of secondary phases in Rb and Cs (Thompson, 1973; Hart et al., 1974; Heinrichs and Thompson, 1976), should be explained by the presence of zeolites in the secondary phases.

6. Concluding remarks

(1) Comparison of the results of dissolution experiments carried out on a basalt glass and forsterite between 150° and 300°C demonstrated a structural (Madelung site energy) control of the release of trace alkalis. The preferential leaching from crystalline silicates (olivines, feldspars, pyroxenes) may strongly affect the composition of hydrothermal springs issuing on the ocean floor.

(2) The distribution coefficients of Li, Rb and Cs between hydrothermal solutions and chlorites, smectites and zeolites have been determined experimentally between 50° and 260°C. For a given cation, the distribution coefficients rank in the same order as the exchange capacities ($D_{\text{zeol.}} > D_{\text{smect.}} > D_{\text{chlor.}}$), whereas, for a given mineral, they increase with decreasing free energies of hydration of cations ($D_{\text{Li}} < D_{\text{Rb}} < D_{\text{Cs}}$). These results, together with the observed decrease of D with increasing temperature, indicate that the distribution of alkalis is mainly controlled by exchange reactions with the compensating cations of the mineral.

(3) From the good agreement observed between computer simulations and analyses of submarine geothermal systems, it is believed that computer experiments can be used successfully to predict the evolution with time of trace elements in solution and mineral assemblages during hydrothermal processes.

Acknowledgements

This research was supported by grants from C.N.R.S. (A.T.P. "Géologie et Géophysique des Océans") and from Commissariat à l'Énergie Atomique. We thank Bernard Reynier (Toulouse) for assistance with the atomic absorption analyses and Christophe Monnin (Toulouse) for his help with computer calculations. We are very grateful to David Crerar (Princeton) and Gil Michard (Paris) for their helpful comments and corrections on the manuscript.

References

Barrer, R.M., 1978. Cation-exchange equilibria in zeolites and felspathoids. In: L.B. Sand and F.A. Mumpton (Editors), Natural Zeolites: Occurrence, Properties, Use. Pergamon, Oxford, pp. 385–395.

Berger, G., 1987. Étude des premiers stades de l'altération hydrothermale de verres basaltiques et d'olivines – Comportement des éléments en trace. Thesis, University of Toulouse III, Toulouse, 132 pp.

Berger, G., Schott, J. and Loubet, M., 1987. Fundamental processes controlling the first stage of alteration of a basalt glass by seawater: an experimental study between 200° and 320°C. Earth Planet. Sci. Lett., 84: 431–445.

Bischoff, J.L. and Seyfried, W.E., 1978. Hydrothermal chemistry of seawater from 25° to 350°C. Am. J. Sci., 278: 838–860.

Caillère, S., Hénin, S. and Rautureau, M., 1982. Minéralogie des argiles. In: INRA (Institut National Recherche Agronomique) — Actualités scientifiques et agronomiques, Vol. 9. Masson, Paris, 159 pp.

Dourgan, W.K., 1974. The absorptiometric determination of aluminum in water – A comparison of some chromogenic reagents and the development of an improved method. Analyst (London), 99: 413–430.

Edmond, J.M., Measures, C., McDuff, R.E., Chan, L.H., Collier, R. and Grant, B., 1979. Ridge crest hydrothermal activity and the balances of the major and minor elements in the ocean: the Galápagos data. Earth Planet. Sci. Lett., 46: 1–18.

Ellis, A.J. and Mahon, W.A.J., 1964. Natural hydrothermal systems and experimental hot-water/rock interactions. Geochim. Cosmochim. Acta, 28: 1323–1357.

Ellis, A.J. and Mahon, W.A.J., 1967. Natural hydrothermal systems and experimental hot water/rock interactions, Part II. Geochim. Cosmochim. Acta, 31: 519–538.

Garofalini, S.H. and Levine, S.M., 1985. Differences in surface behavior of alkali ions in $Li_2O{\cdot}3SiO_2$ and $Na_2O{\cdot}3SiO_2$ glasses. J. Am. Ceram. Soc., 68: 376–379.

Hart, S.R., Erlank, A.J. and Kable, E.J.D., 1974. Seafloor basalt alteration: some chemical and Sr isotopic effects. Contrib. Mineral. Petrol., 44: 219–230.

Heinrichs, S. and Thompson, G., 1976. The low temperature weathering of oceanic basalts by seawater, 2. Trace element fluxes. Geol. Soc. Am., Abstr., 8: 1098.

Helgeson, H.C., Delany, J.M., Nesbitt, H.W. and Bird, D.K., 1978. Summary and critique of the thermodynamic properties of rock-forming minerals. Am. J. Sci., 278: 1–229.

Helgeson, H.C., Kirkham, D.H. and Flowers, G.C., 1981. Theoretical prediction of the thermodynamic behavior of aqueous electrolytes at high pressure and temperatures, IV. Calculation of activity coefficients, osmotic coefficients, and apparent molal and standard and relative partial molal properties to 600°C and 5 kb. Am. J. Sci., 281: 1249–1516.

Ito, J., 1977. Crystal synthesis of a new olivine, $LiScSiO_4$. Am. Mineral., 62: 356–361.

Kester, D.A., Duedall, J.W., Conners, D.M. and Pytkowicz, R.M., 1967. Preparation of artificial seawater. Limnol. Oceanogr., 12: 176–178.

Lagache, M., 1968. Étude expérimentale de la répartition des éléments traces entre la leucite, l'orthose et des solutions hydrothermales – Le rubidium à 600°C. C.R. Acad. Sci. Paris, 267: 141–144.

Lagache, M., 1969. Étude expérimentale de la répartition des éléments traces sodium et césium entre la leucite, l'orthose et des solutions hydrothermales à 600°C. C.R. Acad. Sci., Paris, 268: 1241–1243.

Lagache, M. and Sabatier, G., 1973. Distribution des éléments Na, K, Rb et Cs à l'état de trace entre les feldspaths alcalins et les solutions hydrothermales à 650°C, 1 kbar: données expérimentales et interpretation thermodynamique. Geochim. Cosmochim. Acta, 37: 2617–2640.

Latimer, W.M., Pitzer, K.S. and Slansky, C.M., 1939. The state of the solute in electrolyte solutions. In: R.A. Robinson and R.H. Stokes, Electrolyte Solutions (1959). Butterworths, London, 571 pp.

Martin, J.M. and Whitfield, M., 1983. The significance of the river input of chemical elements to the oceans. In: C.S. Wong, B. Edward, W.B. Kenneth, J.D. Burton and D.G. Edward (Editors), Trace Metals in Seawater. N.A.T.O. (N. Atlantic Treaty Org.) Conf., Ser. Mar. Sci., Vol. 9, Plenum, New York, N.Y., pp. 265–296.

Michard, G., Albarède, F., Michard, A., Minster, J.F., Charlou, J.L. and Tan, M., 1984. Chemistry of solutions from the 13°N East Pacific Rise hydrothermal site. Earth Planet. Sci. Lett., 67: 297–307.

Mottl, M.J., 1983. Metabasalt, axial hot springs, and the structure of hydrothermal systems at mid-ocean ridges. Geol. Soc. Am. Bull, 94: 161–181.

Passaglia, E., 1978. Lattice-constant variations in cation-exchanged chabazites. In: L.B. Sand and F.A. Mumpton (Editors), Natural Zeolites: Occurrence, Properties, Use. Pergamon, Oxford, pp. 45–52.

Roux, J., 1971. Fixation du rubidium et du césium dans la néphéline et dans l'albite à 600°C dans les conditions hydrothermales. C.R. Acad. Sci., Paris, 272: 1469–1472.

Saunders, A.D., Tarney, J., Stern, C.R. and Dalziel, I.W.D., 1979. Geochemistry of Mesozoic marginal basin floor igneous rocks from southern Chile. Geol. Soc. Am. Bull., 90: 237–258.

Schott, J. and Berner, R.A., 1983. X-ray photoelectron studies of the mechanism of iron silicate dissolution during weathering. Geochim. Cosmochim. Acta, 47: 2233–2240.

Schott, J., Berner, R.A. and Sjöberg, E.L., 1981. Mechanism of pyroxene and amphibole weathering I. Experimental studies of iron-free minerals. Geochim. Cosmochim. Acta, 45: 2123–2136.

Seyfried, W.E., 1987. Experimental and theoretical constraints on hydrothermal alteration processes at mid-ocean ridges. Annu. Rev. Earth Planet. Sci., 15: 317–335.

Seyfried, W.E., Janecky, D.R. and Mottl, M.J., 1984. Alteration of the oceanic crust: implications for geochemical cycles of lithium and boron. Geochim. Cosmochim. Acta, 48: 557–569.

Staudigel, H. and Hart, S.R., 1983. Alteration of basaltic glass: mechanisms and significance for the oceanic crust–seawater budget. Geochim. Cosmochim. Acta, 47: 337–350.

Stoffyn-Egli, P. and Mackenzie, F.T., 1984. Mass balance of dissolved lithium in the oceans. Geochim. Cosmochim. Acta, 48: 859–872.

Thompson, G., 1973. A geochemical study of the low-temperature interaction of seawater and oceanic igneous rocks. Eos (Trans. Am. Geophys. Union), 54: 1015–1019.

Tlig, S., 1982. Géochimie des sédiments de l'Océan Indien et l'Océan Pacifique - Intérêt du fractionnement minéralogique et de l'étude de plusieurs groupes d'éléments dosés par activation neutronique. Thesis, University of Paris-Sud, Orsay, 270 pp.

Volfinger, M., 1970. Partage de Na et Li entre sanidine, muscovite et solution hydrothermale à 600°C, 1000 bars. C.R. Acad. Sci. Paris, 271: 1345–1347.

Volfinger, M., 1974. Effet de la composition des micas trioctaédriques sur les distributions de Rb et Cs à l'état de traces. Earth. Planet. Sci. Lett., 24: 299–309.

Volfinger, M., 1976. Effet de la température sur les distributions de Na, Rb et Cs entre la sanidine, la muscovite, la phlogopite et une solution hydrothermale sous pression de 1 kb. Geochim. Cosmochim. Acta, 40: 267–282.

Volfinger, M. and Robert, J.L., 1980. Structural control of the distribution of trace elements between silicates and hydrothermal solutions. Geochim. Cosmochim. Acta, 44: 1455–1461.

Von Damm, K.L., Edmond, J.M., Grant, B.C., Measures, C.I., Walden, B. and Weiss, R., 1985. Chemistry of submarine hydrothermal solutions at 21°N East Pacific Rise. Geochim. Cosmochim. Acta, 49: 2197–2220.

Wolery, T.J., 1979. Calculation of chemical equilibrium between aqueous solution and minerals: the EQ3/6 software package. UCRL-52658, Lawrence Livermore Natl. Lab., Livermore, Calif.

Wolery, T.J., 1983. EQ3NR, a computer program for geochemical aqueous speciation–solubility calculations. UCRL-5, Lawrence Livermore Natl. Lab., Livermore, Calif.